Supporting information

New analogs of the complement C3 inhibitor compstatin with increased solubility and improved pharmacokinetic profile

Nadja Berger[†], Tchilabalo Dilezitoko Alayi[†], Ranillo R. G. Resuello[‡], Joel V. Tuplano[‡], Edimara S. Reis[†], John D. Lambris*[,†]

[†]Department of Pathology and Laboratory Medicine, Perelman School of Medicine, University of Pennsylvania, Philadelphia, PA 19104, USA

[‡]Simian Conservation Breeding and Research Center (SICONBREC), Makati City, 1231, Philippines

Table of contents

	Page
Figure 1. Complement inhibitory potency of new Cp40 analogs.	S2
Figure 2. Kinetic analysis of the new Cp40 analogs.	S3
Figure 3. Comparative profiles of the binding of Cp40 analogs to C3b.	S4
Figure 4. Quantification of peptide cleavage fragments in the plasma of NHPs.	S5
Figure 5. Analytical RP-HPLC showing the retention times of the Cp40 analogues.	S6-S8
Figure 6. MALDI spectra of the new PEGylated Cp40 analogs.	S9
Figure 7. MALDI spectra of the new Cp40-Lysine analogs.	S10

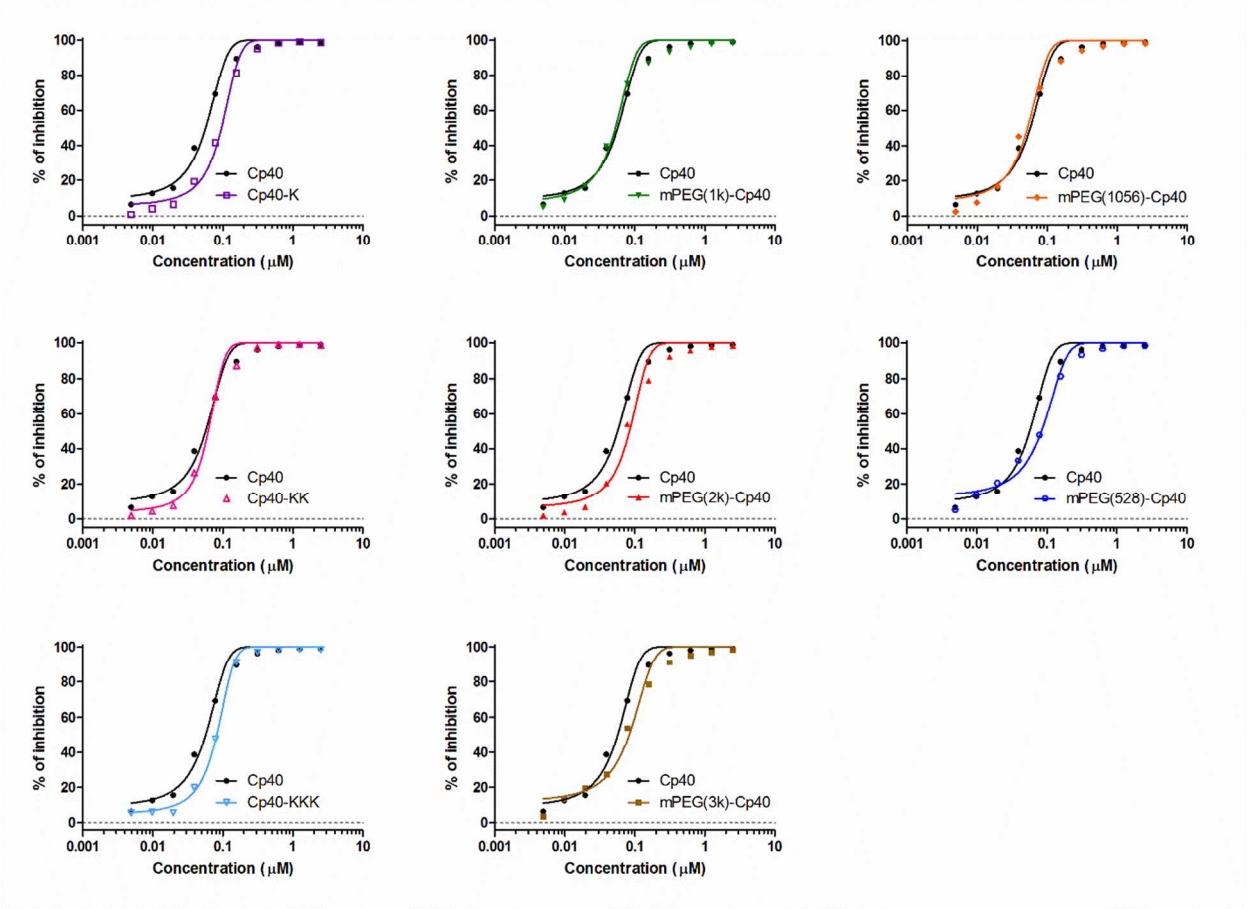

Supplemental Figure 1. Complement inhibitory potency of new Cp40 analogs. Inhibition of the classical pathway activation by increasing concentrations of Cp40 analogues was determined in normal human plasma incubated with immune-complexes. Complement inhibition in response to Cp40 is shown in each graph for comparison. Graphs depict a representative experiment from three independent experiments.

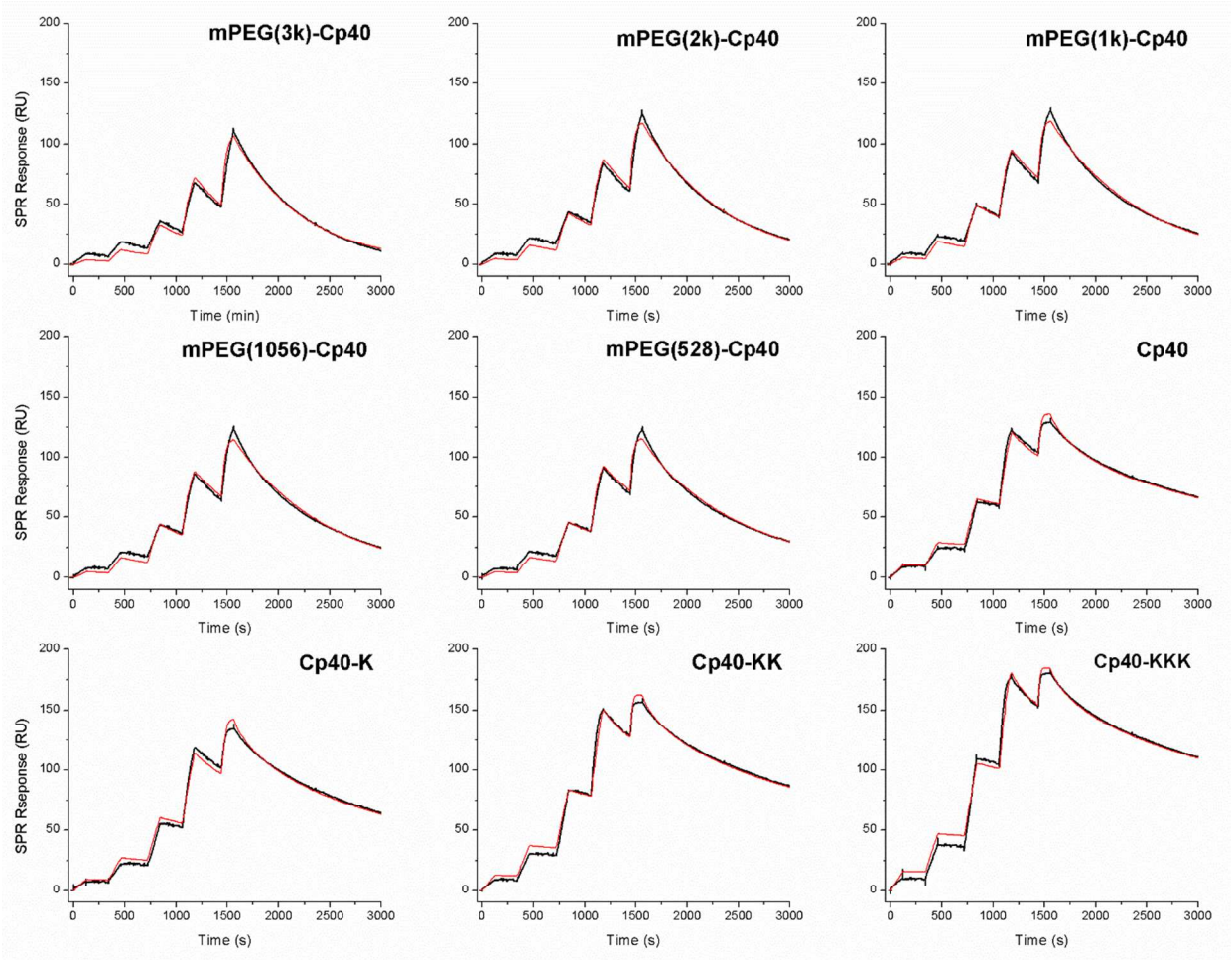

Supplemental Figure 2. Kinetic analysis of the new Cp40 analogs. Each SPR sensorgram shows representative data from three independent experiments with a single-cycle kinetic titration of an individual peptide over five concentrations (black: processed SPR data; red: kinetic fit to 1:1 Langmuir model).

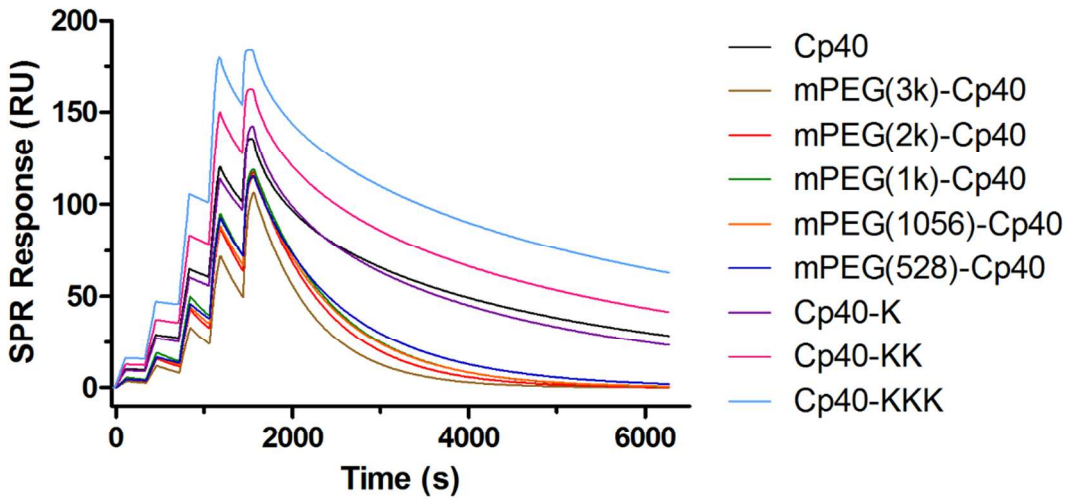

Supplemental Figure 3. Comparative profiles of the binding of Cp40 analogs to C3b, as assessed by SPR experiments after fitting to a 1:1 Langmuir binding model.

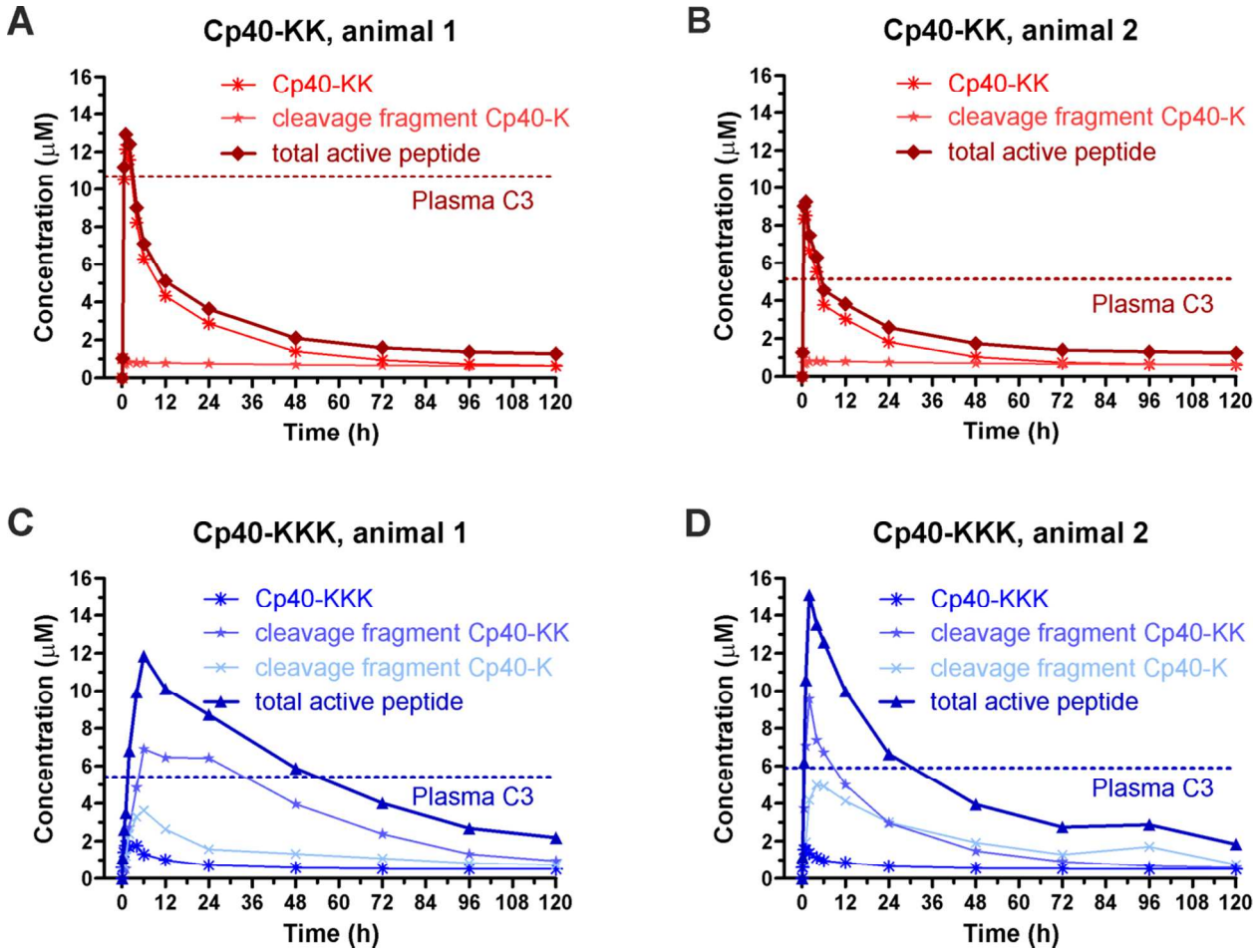

Supplemental Figure 4. Quantification of peptide cleavage fragments in the plasma of cynomolgus monkeys. Animals (n = 2 per treatment group) were injected with 2 mg/kg of Cp40-KK (A, B) or Cp40-KKK (C, D). The injected peptides were cleaved *in vivo* generating Cp40-K and Cp40-KK cleavage fragments. Concentration of peptides was determined by UPLC-ESI-MS. Graphs depict the plasma concentrations of cleavage fragments; i.e.; Cp40-K in A, B and Cp40-KK and Cp40-K in C, D as well as the total concentration of active peptides.

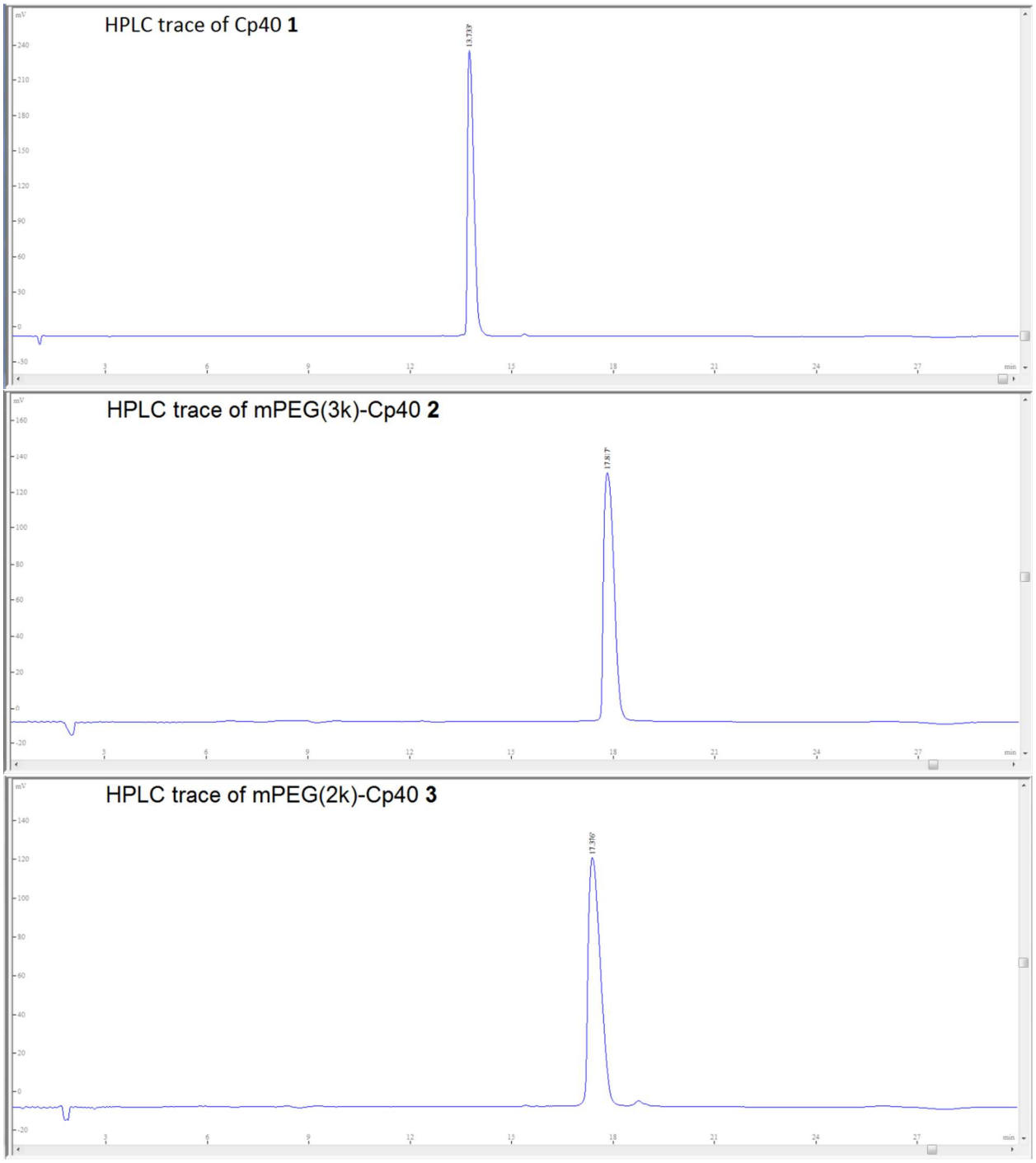

Supplemental Figure 5. Analytical RP-HPLC showing the retention times of the Cp40 analogues. Cp40 **1**, mPEG(3k)-Cp40 **2**, and mPEG(2k)-Cp40 **3**. Conditions: Waters XBridge BEH C18 5 µm (150x4.6 mm) column eluting at a flow rate of 2.5 mL/min and a gradient of 5-70% buffer B (0.1% TFA in CH_3CN) in buffer A (0.1% TFA in H_2O) over 22 min.

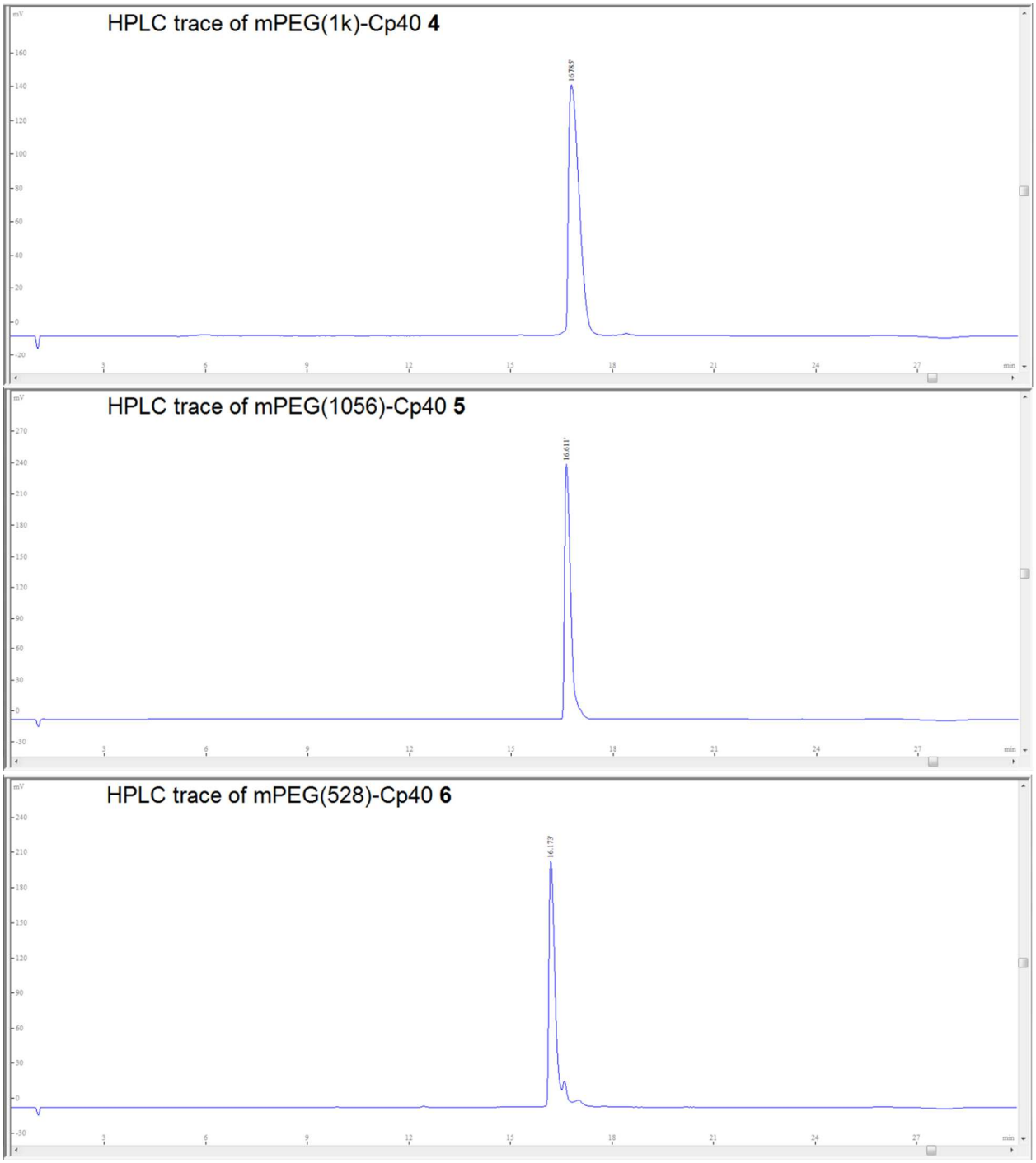

Supplemental Figure 5. Analytical RP-HPLC showing the retention times of purified mPEG(1k)-Cp40 **4**, mPEG(1056)-Cp40 **5**, and mPEG(528)-Cp40 **6**. Conditions: Waters XBridge BEH C18 5 µm (150x4.6 mm) column eluting at a flow rate of 2.5 mL/min and a gradient of 5-70% buffer B (0.1% TFA in CH_3CN) in buffer A (0.1% TFA in H_2O) over 22 min.

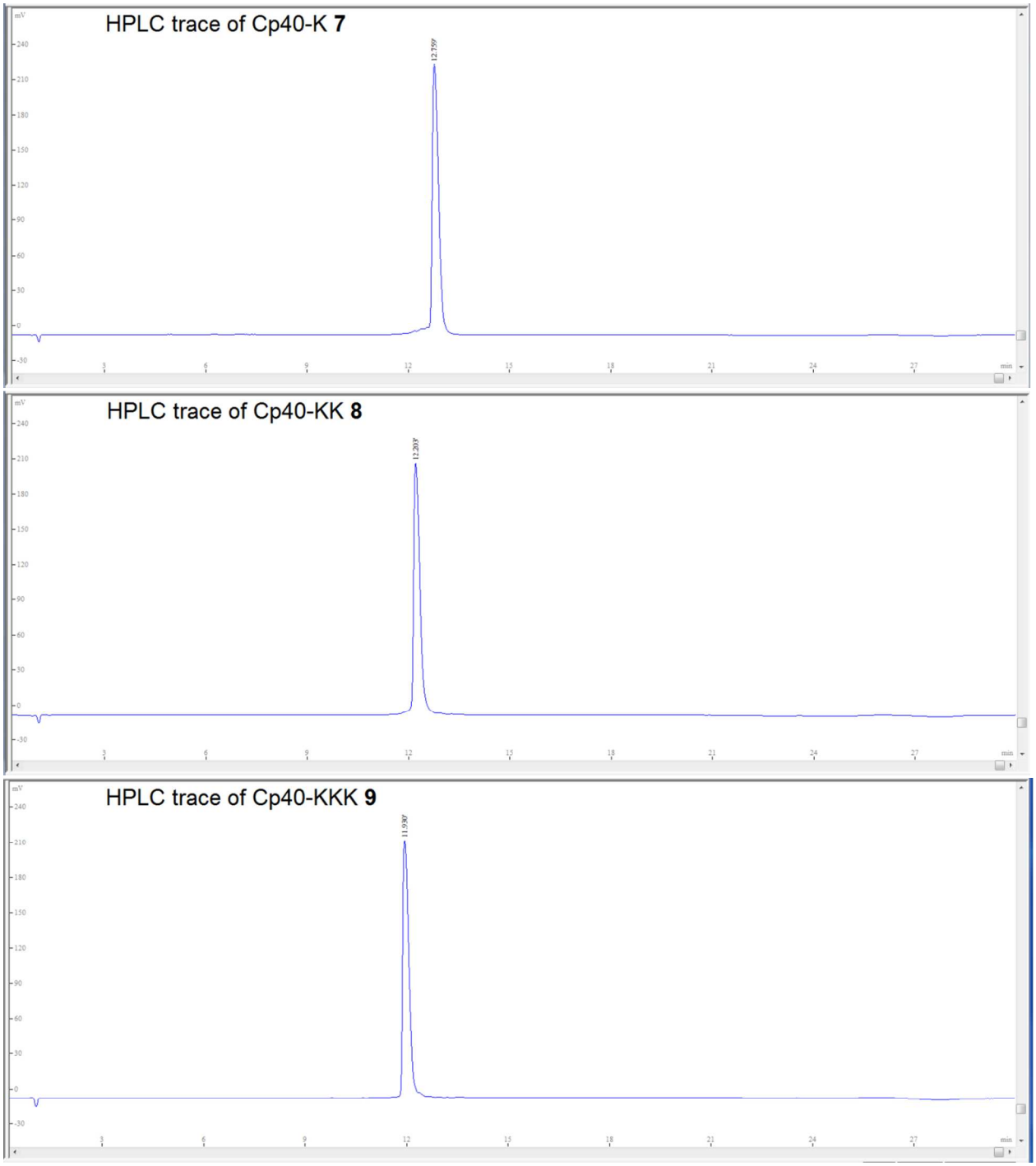

Supplemental Figure 5. Analytical RP-HPLC showing the retention times of purified Cp40-K **7**, Cp40-KK **8**, and Cp40-KKK **9**. Conditions: Waters XBridge BEH C18 5 µm (150x4.6 mm) column eluting at a flow rate of 2.5 mL/min and a gradient of 5-70% buffer B (0.1% TFA in CH_3CN) in buffer A (0.1% TFA in H_2O) over 22 min.

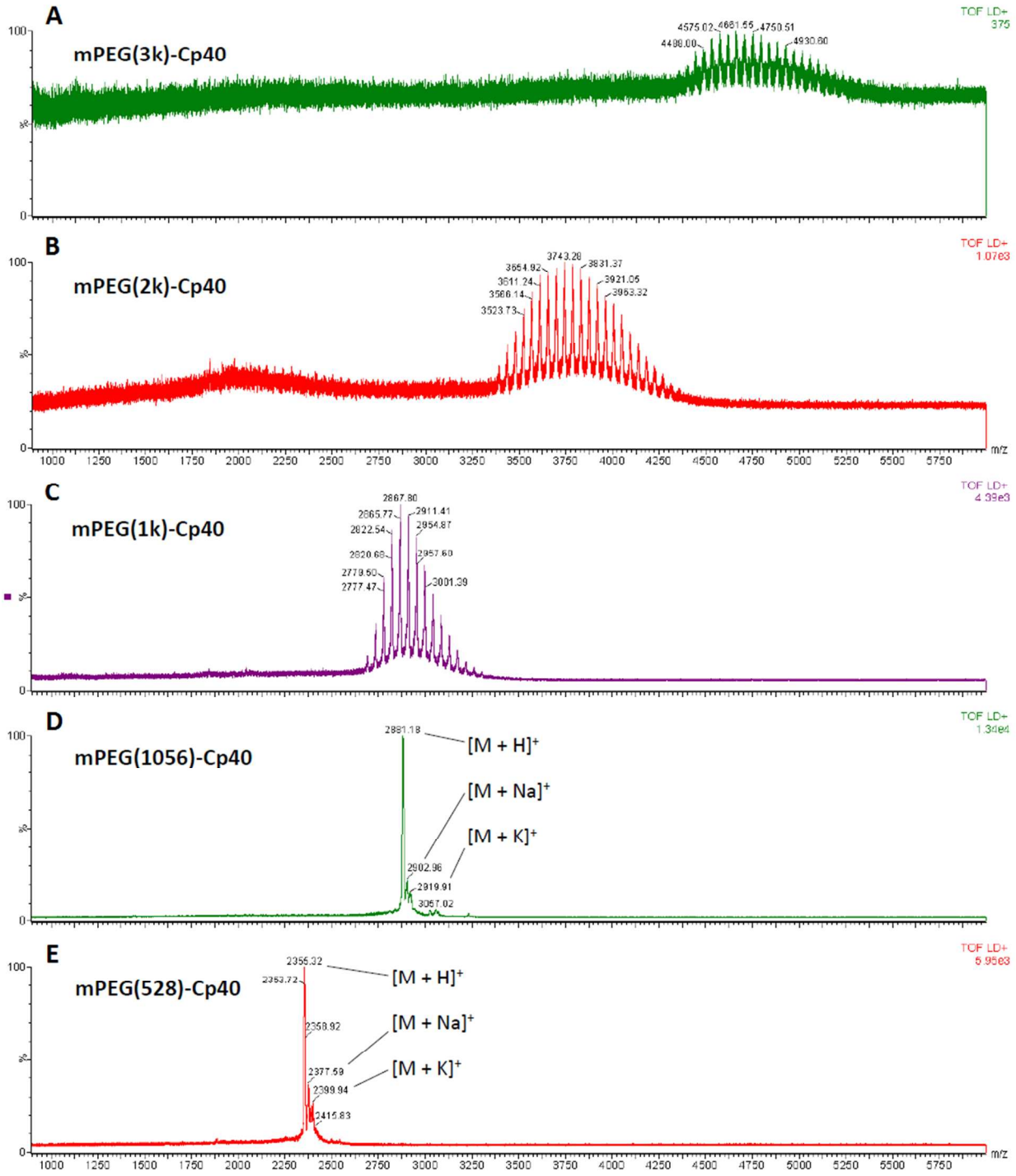

Supplemental Figure 6. MALDI spectra of the new PEGylated Cp40 analogs. (A) polydisperse mPEG(3k)-Cp40, (B) polydisperse mPEG(2k)-Cp40, (C) polydisperse mPEG(1k)-Cp40, (D) monodisperse mPEG(1056)-Cp40, (E) monodisperse mPEG(528)-Cp40.

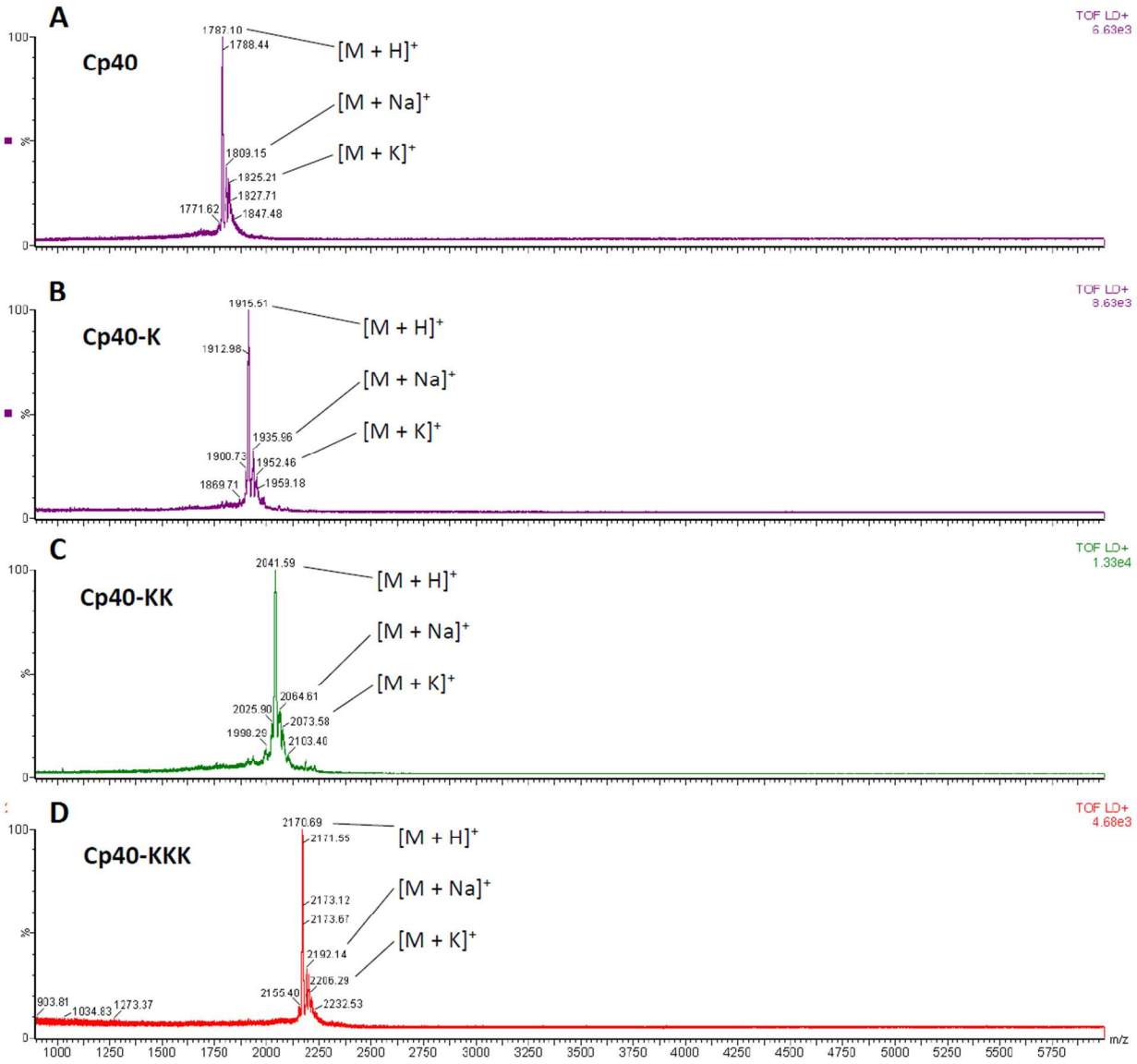

Supplemental Figure 7. MALDI spectra of the new Cp40-Lysine analogs. (A) Cp40, (B) Cp40-K, (C) Cp40-KK, (D) Cp40-KKK.